

AIR-BREATHING PULSED DETONATION ENGINE  
THRUST MODULE: NUMERICAL SIMULATIONS,  
FIRE TESTS, AND FLIGHT EXPERIMENTS

S. M. Frolov<sup>1,2,3</sup>, V. S. Aksenov<sup>1,2</sup>, V. S. Ivanov<sup>1,2,3</sup>,  
I. O. Shamshin<sup>1,2,3</sup>, and A. E. Zangiev<sup>1</sup>

<sup>1</sup>Semenov Institute of Chemical Physics  
Russian Academy of Sciences, Moscow, Russia  
e-mail: smfrol@chph.ras.ru

<sup>2</sup>National Research Nuclear University MEPhI  
Moscow, Russia

<sup>3</sup>Scientific Research Institute for System Analysis  
Russian Academy of Sciences  
Moscow, Russia

The thrust module (TM) for an aircraft designed for a subsonic flight at a speed of 30 to 120 m/s when operating on a standard aviation kerosene TS-1 was developed using the analytical estimates and parametric multivariant three-dimensional (3D) calculations. The TM consists of an air intake with a check valve, a fuel supply system, a prechamber-jet ignition system, and a combustion chamber with an attached detonation tube. An experimental sample of TM was fabricated and its fire tests were carried out on a test rig with a thrust-measuring table. In fire tests, TM characteristics are obtained in the form of dependencies of effective thrust, aerodynamic drag, and fuel-based specific impulse on fuel consumption at different speeds of the approaching air flow. It has been experimentally shown that the fuel-based specific impulse of the TM reaches 1000–1200 s, and the effective thrust developed by it reaches 180–200 N. The results of catapult launching tests of an unmanned aerial vehicle (UAV) powered with one and two paired TMs are also presented. The autonomous flight of the UAV with a new type of power plant is demonstrated.

---

DOI: 10.30826/ICPCD201826 ©The authors, published by TORUS PRESS

## 1 Introduction

In existing ramjets, a stationary operation process with continuous conversion of the chemical energy of fuel into the useful work of expanding products of deflagrative (subsonic) combustion is used. Continuous combustion of fuel in the combustor is ensured by special means and/or devices preventing flame blow-off and proceeds with a significant decrease in density (by a factor of 2 to 5) and with a slight decrease in pressure (by several percent) in the combustion products. Ramjets with pulsating (nonstationary) deflagrative combustion are often considered as an alternative to the ramjets with continuous deflagrative combustion of fuel. Such ramjets equipped with resonator tubes operate on the self-oscillating combustion of fuel with a significant decrease in density, but with a slight (by several percent) increase in pressure\*. A well-known example is German V-1 vehicle of the Second World War.

Since 1940–1950s, thanks to the works of Ya. B. Zel'dovich [1] and B. V. Voitsekhovskii [2], a new idea arose that is the possibility of using detonative (supersonic) rather than deflagrative combustion of fuel in ramjets with the implication that the detonative combustion theoretically promises a significant increase in the energy efficiency. In contrast to stationary deflagrative combustion, in which the density and pressure of the products of chemical transformations decrease, in stationary detonative combustion, the density and pressure of reaction products increase substantially (density increases by a factor of 2, and pressure increases by a factor of 15–17). Since stationary detonative combustion of fuel in an oblique detonation wave is accompanied by large entropy losses [1], the possibility of organizing detonative combustion in propagating detonation waves was considered: either in a continuous “spinning” detonation wave [2,3] or in a pulse-periodic detonation wave [4]. Engines with continuous spinning detonation of fuel are currently called continuous-detonation engines (CDEs), and engines with pulse-periodic detonations are referred to as pulsed detonation engines (PDEs). The combustion chamber in a CDE is made, as a rule, in the form of an annular chamber with axial air supply and with a distributed radial fuel supply by multiple jets. The spinning

---

\*The latter does not contradict the laws of conservation of mass and momentum, since the workflow in such an engine is nonstationary.

detonation wave continuously rotates in the annular gap downstream from the fuel jet holes, thus burning all the fuel entering the combustor during one turn of the wave around the engine axis, and the detonation products continuously expell into the ambient atmosphere through the nozzle, thus creating continuous thrust. The combustion chamber in the PDE is made, as a rule, in the form of a straight duct, periodically filled with fuel–air mixture and equipped with a mechanical check valve periodically blocking air access to the combustor. During the period when the valve is closed, a detonation wave runs along the duct, thus burning all the fuel accumulated in the combustor, and the detonation products expell into the ambient atmosphere through the nozzle, creating a pulse of thrust.

This paper is a continuation of the studies described in [5]. In [5], fire tests of the PDE model with a mechanical check valve were conducted in a subsonic wind tunnel with a free air jet of the Mach number ranging from 0.65 to 0.85. Liquid propane was used as a fuel. Operating modes with a frequency of up to 10 Hz, an average thrust of up to 30 N, and an average specific impulse of up to 1000 s were obtained. The purpose of further research is the development, based on the results of [5], of a pulsed-detonation liquid-fuel (standard aircraft kerosene TS-1) TM with a fuel-based specific impulse of at least 1000 s. The TM is designed for testing in subsonic flight conditions as a part of an aircraft model equipped with wings.

## 2 Assessment of Integral Performance

Figure 1 shows a schematic diagram of the pulsed-detonation TM. The TM is a straight channel with specified cross-sectional area and length. It consists of an air intake combined with a check valve; a fuel supply system; an ignition system; a combustor where fuel is mixed with air and ignited; a detonation tube; and an outlet device (nozzle). The detonation tube consists of the flame acceleration section with turbulizing obstacles of a special shape. The design of the tube sections and the details of their integration as well as the shape and arrangement of turbulizing obstacles are the subjects of patenting and are not discussed here. Currently, the operation frequency of the TM is limited by the response time of the mechanical check valve: the

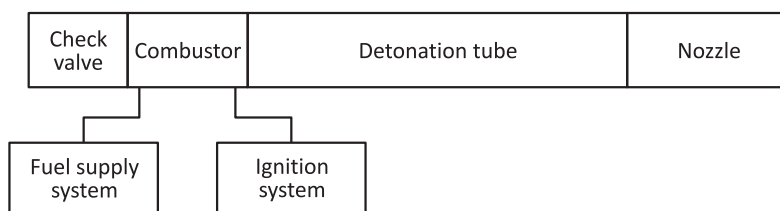


**Figure 1** Schematic diagram of the TM

maximum frequency is  $\sim 20$  Hz. The operation cycle includes filling the combustor and the detonation tube with the fuel–air mixture while the check valve is open, then igniting the mixture, closing the check valve (actively or passively), deflagration-to-detonation transition (DDT), burning the fuel–air mixture in the propagating detonation wave, and expelling the detonation products through the nozzle into the ambient atmosphere. At the stages of combustion of fuel–air mixture and the expelling of detonation products through the nozzle, a static overpressure is maintained on the inner surface of the closed check valve, which creates the force acting against the approaching air flow, the thrust force. When the static pressure at the check valve drops to the level of the total pressure of the approaching air flow, the check valve is opened and the operation cycle of the TM repeats.

The base fuel for the TM is the standard aviation kerosene TS-1.

To estimate analytically the expected integral performance of the TM (operation frequency  $f$ , full thrust  $T$ , effective thrust  $F$ , and aerodynamic drag  $R$ ), the calculations were made for a TM of length  $L$  ranging from 1 to 3 m with a square cross section of  $100 \times 100$  mm (corresponding to a cross section of a round tube of 113 mm in diameter) at different flight speeds. A scheme of the TM without an exit nozzle was considered. Calculations are based on the following formulae:

$$f = \frac{VC_{\text{in}}}{L};$$

$$T = \dot{m}_f I_{\text{sp}} g, \quad \dot{m}_f = \rho V S Y_{\text{st}} C_{\text{in}} C_f;$$

$$F = T + R, \quad R = -\frac{C_X S \rho V^2}{2}$$

where  $V$  is the flight speed;  $C_{in}$  is the discharge coefficient of the intake with a check valve;  $\dot{m}_f$  is the fuel consumption;  $I_{sp}$  is the fuel-based specific impulse;  $g$  is the acceleration of gravity;  $\rho$  is the air density;  $S$  is the cross-sectional area of the TM;  $Y_{st}$  is the fuel mass fraction in the stoichiometric kerosene–air mixture;  $C_f$  is the fuel fill factor of the TM; and  $C_X$  is the aerodynamic drag coefficient of the TM. Forces  $T$ ,  $F$ , and  $R$  are treated as positive if they are directed opposite to the approaching air flow.

The calculations are based on the following values of the governing parameters and coefficients:  $I_{sp} = 1000$  s (obtained experimentally in [5]);  $C_X = 1.0$ ,  $Y_{st} = 0.06$ ;  $C_{in} = 0.5$  (i. e., 50% of the approaching air flow enters the intake, the losses are due to the presence of baffles in the design of the check valve and with the pressure loss associated with air purging through the engine path);  $C_f = 0.8$  (i. e., the detonation tube is filled with the fuel–air mixture during 80% of the cycle time, whereas the remaining 20% of the cycle time are used for the mixture to burn out and the detonation products to expel from the engine).

Figures 2 and 3 show the results of calculations in the form of the  $f(V)$  curves at  $L = 1, 2$ , and 3 m (see Fig. 2) and in the form of dependencies  $T(V)$ ,  $F(V)$ , and  $S(V)$  at  $L = 3$  m (see Fig. 3). In view of the current limitations imposed on the check valve in terms of the

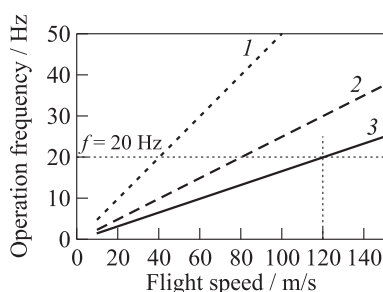


**Figure 2** Calculated dependencies of the operation frequency on the flight speed for the TM of different lengths: 1 —  $L = 1$  m; 2 —

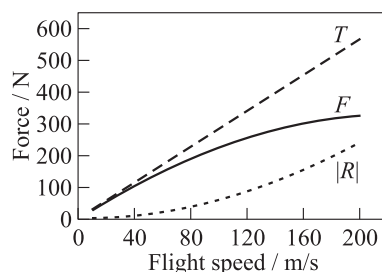


**Figure 3** Calculated thrust parameters vs. flight speed for the 3-meter long TM with  $100 \times 100$  mm cross-sectional area

maximum operation frequency (20 Hz), there is a limiting flight speed at which the maximum effective thrust of the TM can be attained: in the 3-meter long TM, it is possible to realize an operation process at a flight speed of up to 120 m/s (see Fig. 2) with an effective thrust at the sea level up to 250 N (see Fig. 3). In the 2-meter long TM, the maximum speed of flight at the same operating frequency is 80 m/s.

### 3 Design of the Thrust Module

The design of the TM was created using multivariant numerical calculations applying a technique described, e. g., in [6]. The operation process in the TM was simulated in the 3D approximation. The underlying mathematical model is based on the Unsteady Reynolds-Averaged Navier–Stokes (URANS) equations of conservation of mass, momentum, and energy for a nonstationary compressible turbulent reacting flow. The turbulent fluxes of mass, momentum, and energy were simulated using the  $k$ - $\varepsilon$  model of turbulence ( $k$  is the kinetic energy of turbulence and  $\varepsilon$  is its dissipation). Simulation of chemical sources during turbulent combustion and DDT required consideration of the contributions of both frontal combustion and volumetric preflame reactions. For their determination, the Flame Tracking algorithm for the explicit tracking of the flame front was used and the contributions of the volumetric reactions were determined using the Particle method [6]. Turbulent burning of kerosene vapor was simulated using a database of the laminar flame properties in kerosene–air mixtures [7]. Self-ignition of kerosene vapor was described either by the detailed kinetics of oxidation of the surrogate fuel simulating kerosene or by a simplified single-stage reaction with variable Arrhenius parameters for low- and high-temperature oxidation [8].

The set of governing equations supplemented by the  $k$ - $\varepsilon$ -model of turbulence and the conjugate Flame Tracking–Particle model was closed by the caloric and thermal equations of state of an ideal gas with variable specific heats as well as by initial and boundary conditions. All thermophysical parameters of the gas were considered variable. For a numerical solution, we used a method based on the finite-volume discretization of the equations with the first order of approximation in space and in time. To avoid excessive mesh re-

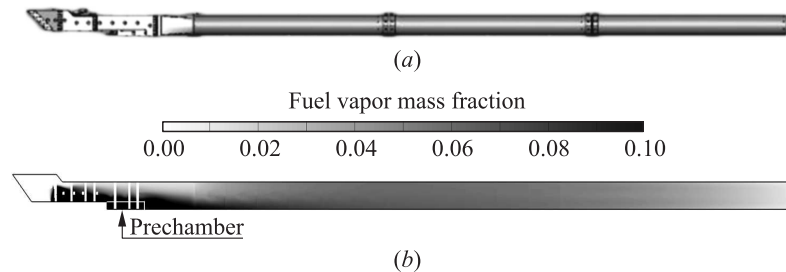


**Figure 4** The 3D model of TM (a) and an example of the calculated field of fuel vapor mass fraction in the inner path of the TM at the end of the filling stage of the detonation tube with a combustible mixture (check valve is open) (b)

finement near solid surfaces, the standard wall functions were used. The baseline computational mesh consisted of 800,000 cells. The effect of the dimensions of the computational cells on the flow structure was checked by additional calculations on essentially smaller meshes.

Calculations were performed for the conditions when the TM is placed in a free air stream with the approaching flow velocity of 10 m/s with the injection of liquid kerosene into the combustor. As a result of the calculations, a 3-meter long TM with a square-circular cross section is designed (Fig. 4a): the intake and combustor have a square section of  $100 \times 100$  mm and the detonation tube is made in the form of a round tube with a diameter of 100 mm. The exit nozzle is absent. The specified parameters of the TM are close to the parameters adopted in the analytical estimates of section 2. With the help of parametric 3D calculations, the best length of the combustor is selected, which ensures efficient mixing of fuel with air. Also, the best method of ignition (prechamber-jet ignition), the best location of the prechamber, the minimum length of the section with turbulizing obstacles for accelerating the flame and ensuring DDT, and the best degree of filling the detonation tube with the fuel-air mixture for achieving the maximum completeness of combustion are determined. The design and operation mode of the TM for attaining the minimum pressure loss and the maximum thrust were not optimized.

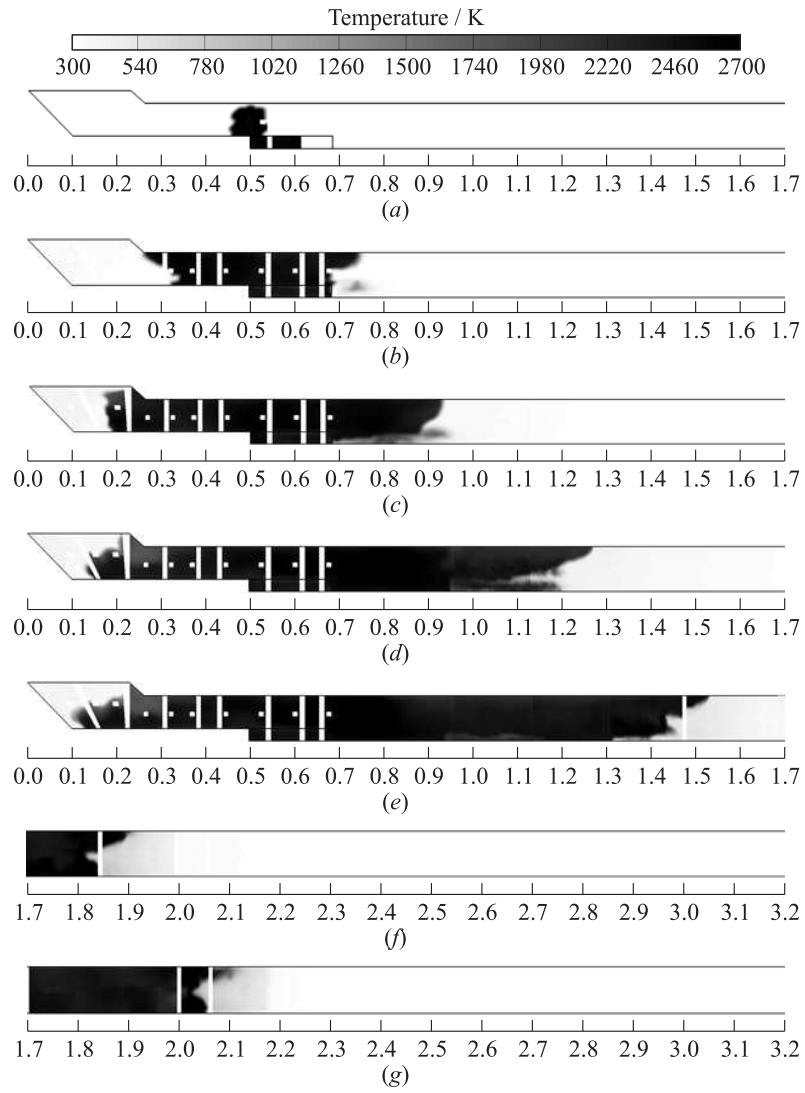


**Figure 5** The calculated gas temperature field in the middle longitudinal section of the inner path of the TM path at different time instants after prechamber ignition (check valve is closed): (a) 3 ms; (b) 5; (c) 6; (d) 7; (e) 7.5; (f) 8; and (g) 8.25 ms (*to be continued*)

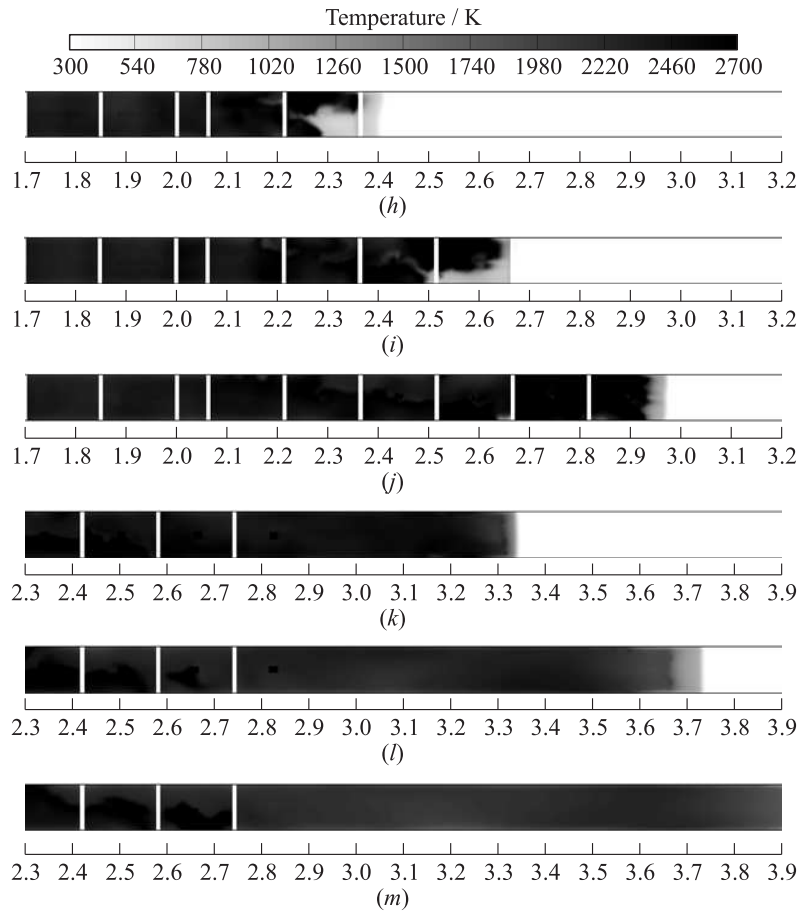


**Figure 5** (*continued*) The calculated gas temperature field in the middle longitudinal section of the inner path of the TM path at different time instants after prechamber ignition (check valve is closed): (h) 8.5 ms; (i) 8.75; (j) 9; (k) 9.25; (l) 9.5; and (m) 9.75 ms

As an example of calculation, Fig. 4b shows the calculated field of fuel vapor mass fraction in the inner path of the TM at the end of the stage of filling the detonation tube with the fuel-air mixture. In the prechamber and its surroundings, the fuel mixture is seen to be

enriched with fuel, whereas in the detonation tube, the composition of the fuel–air mixture is close to stoichiometric ( $\approx 6\%$ ). At the end of the detonation tube, the fuel–air mixture is seen to be fuel-lean due

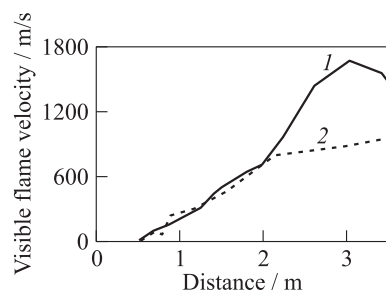


**Figure 6** Comparison of calculated dependencies of the apparent flame front velocity on the traversed (axial) distance for two variants of the TM: 1 — with DDT; and 2 — without DDT

to incomplete filling and due to admixing of the purging air, which separates the fresh reacting mixture from the combustion products of the previous cycle.

Another example of calculation is shown in Fig. 5 in the form of the calculated temperature fields in the inner path of the TM at different time instants after the ignition of the fuel–air mixture. The ignition was simulated by placing a hot flame kernel with a diameter of 3 mm behind the ledge of

the prechamber. In this example, the DDT is reached at the end of the last section of the detonation tube with the turbulizing obstacles. Figure 6 compares the calculated dependencies of the visible flame front velocity on the traversed (axial) distance for two variants of the TM: with and without DDT. In the first case, the turbulizing obstacles provide flame acceleration to 900–1000 m/s at the shortest distance (2.2–2.3 m), followed by a fast DDT [9] and the propagation of the detonation wave in the smooth section of the detonation tube. In the second case, the shape and arrangement of the turbulizing obstacles did not provide DDT. The decrease in the detonation velocity in the end section of the detonation tube is explained by the incomplete and inhomogeneous filling of the tube with the fresh fuel–air mixture (see Fig. 4b).

## 4 Test Bench

An experimental sample of the TM (hereinafter, TM) manufactured in accordance with the 3D model of Fig. 4a was installed on a test

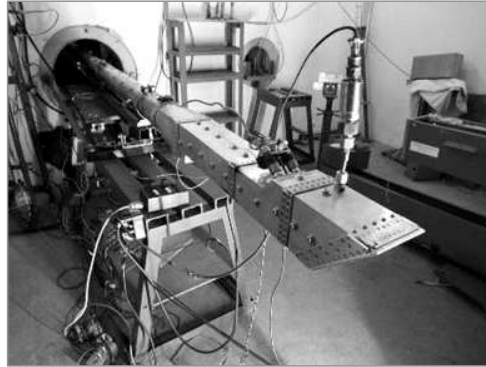


**Figure 7** Photo of the TM installed on the test bench

bench located in an armored chamber (Fig. 7). The combustor of the TM with the check valve of the petal type is made of aluminum AD31. Kerosene was fed to the combustor using two automotive BOSCH injectors at an angle of  $45^\circ$  to the combustor axis. The sections with turbulizing obstacles and the smooth section of the detonation tube are made of stainless steel 12X18N9T (tube 100x1). The turbulizing obstacles are also made of stainless steel. There is no provision for forced cooling of the TM: in fire tests with an operation frequency of up to 14 Hz, the temperature of combustor walls did not exceed  $200^\circ\text{C}$  and the maximum recorded temperature of the turbulizing obstacles was  $700^\circ\text{C}$ .

The approaching air flow was obtained using a SCL-K11TS turbo-blower providing an air flow velocity of 20 to 100 m/s in a free jet. The speed of the air flow was measured with a Pitot tube installed in the air supply duct. When the air was switched on and off, the zero lines for the thrust force and the aerodynamic drag of the TM were determined.

For the supply of liquid fuel, a displacement system with a 3-liter fuel tank mounted on the balance was used. As a displacing gas, nitrogen was used with a displacement pressure up to 70 atm. A pressure sensor is installed in the fuel supply system. To determine the fuel mass flow rate provided by the fuel supply system in the TM (including the injectors), a series of preliminary calibration tests

was performed in the displacement pressure range of 8 to 65 atm. According to the results of the tests, the graphical dependence of the fuel consumption on the displacement pressure has been obtained.

The data acquisition system of the operation process in the TM included two ionization probes, a low-frequency pressure sensor, and a load cell. Two ionization probes installed in a smooth section of the detonation tube at a distance of 330 mm from each other determined the presence of the detonation wave and (indirectly) the degree of filling the detonation tube with a combustible mixture. The pressure sensor was installed closely behind the check valve to record the dynamics of static pressure variation on the thrust wall (with the check valve closed) and the thrust force created by the TM was estimated based on its record. The thrust force created by the TM was also measured directly by the Tenzo-M T2-200 load cell mounted on the thrust table of the test bench.

Figure 8 shows an example of primary records of the ionization probes (curves 1 and 2 in Fig. 8a) and the pressure sensor (Fig. 8b) in a typical single cycle during a fire test of the TM operating at a frequency of 4 Hz. Using the time delay between the signals of

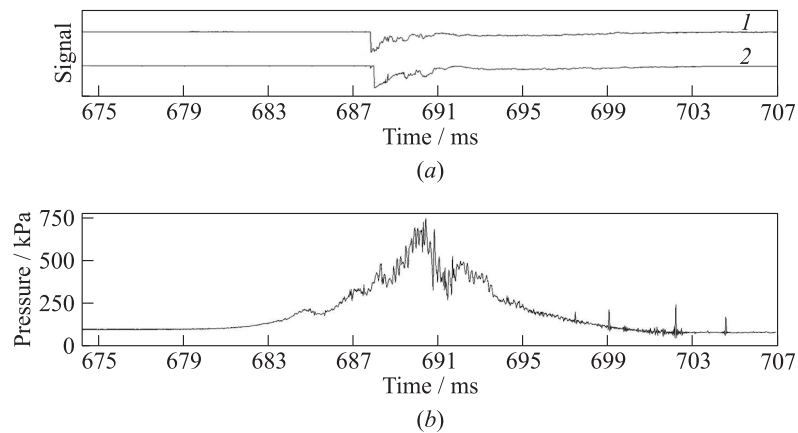


**Figure 8** Example of primary records of ionization probes (curves 1 and 2) (a) and a low-frequency pressure sensor at the check valve (b) in a fire test of TM with an operation frequency of 4 Hz

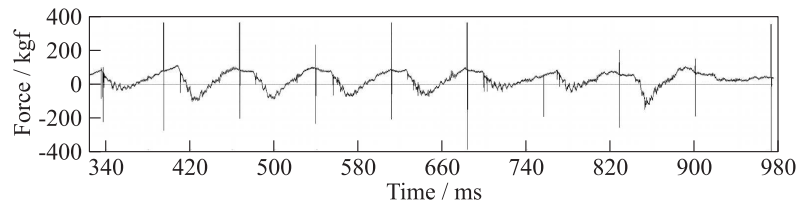


**Figure 9** An example of a primary record of a load cell in 10 successive cycles of a fire test at an operation frequency of 14 Hz

the ionization probes, it is easy to determine the detonation velocity:  $\sim 1800$  m/s. The maximum absolute static pressure at the check valve in the cycle under consideration is  $\sim 700$  kPa, with the maximum being achieved after the detonation wave exits the detonation tube (see Fig. 8b). The duration of the overpressure signal on the check valve is about 17 ms.

Figure 9 shows an example of a primary record of a load cell in 10 cycles of a fire test of the TM at an operation frequency of 14 Hz. Oscillations with an amplitude up to 100 N are observed on the record. The average thrust of the TM was determined by integrating the thrust dependence on time for a time interval of at least 10 s and a number of pulses of at least 50.

## 5 Results of Fire Tests

The objective of fire tests was to obtain the thrust characteristics of the TM at various speeds of the approaching air flow. The obtained results are planned to be used when performing flight tests of the TM as a part of the aircraft model. Figure 10 shows examples of thrust characteristics of the TM in terms of the dependencies of the effective thrust, aerodynamic drag, and fuel-based specific impulse on the fuel consumption for the speed of the approaching air flow  $V = 65$  m/s. The effective thrust of the TM is positive and increases with fuel consumption and with operation frequency (see Fig. 10a). The maximum effective thrust in Fig. 10a ( $F = 50$  N) is reached at operation frequency  $f = 14$  Hz. The measured aerodynamic drag of the TM  $R = -30$  N. If one compares the indicated measured values of the effective thrust and aerodynamic drag with the values depicted in

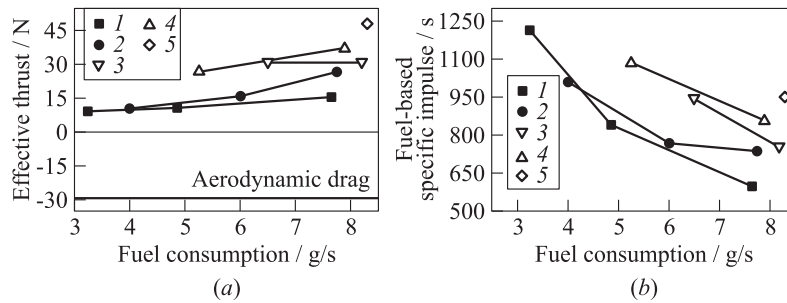


**Figure 10** Examples of measured thrust characteristics of the TM in terms of the dependencies of effective thrust and aerodynamic drag (a) and fuel-based specific impulse (b) on fuel consumption at the speed of the approaching air flow  $V = 65$  m/s: 1 —  $f = 4$  Hz; 2 — 5; 3 — 6.7; 4 — 10; and 5 —  $f = 14$  Hz

Fig. 3 at  $V = 65$  m/s, it turns out that the measured effective thrust is three times smaller than the calculated value (150 N), while the measured and calculated values of the aerodynamic drag are the same. Such a significant difference in the values of  $F$  can be associated with a low discharge coefficient of the intake with a check valve,  $C_{in}$ , in the experimental sample of the TM: instead of a value of 0.5 taken in the calculations, its real value seems to be three times smaller, i. e.,  $C_{in} \approx 0.17$ . To increase the discharge coefficient  $C_{in}$  and, consequently, the effective thrust  $F$ , it is necessary to undertake proper measures to reduce the blockage of the cross section of the intake by the valve and other structural elements, i. e., to solve the task on optimization of the design of the internal path of the TM not only for ensuring the operation process, but also for minimizing the pressure loss.

As for the fuel-based specific impulse (see Fig. 10b), when the TM operates at a frequency of 4–5 Hz at low fuel consumption (3–4 g/s), the measured fuel-based specific impulse is at the level of 1000–1200 s, which is close to the value, presumed in the calculations (1000 s). With the increase in fuel consumption at a fixed operation frequency, the measured fuel-based specific impulse decreases because a part of the fuel expels from the detonation tube into the ambient atmosphere and does not participate in the operation process. Si-

multaneous increase in the operation frequency to  $f = 10$  Hz and fuel consumption to 5–6 g/s leads to an increase in the fuel-based specific impulse to 1000–1100 s. At a frequency of  $f = 14$  Hz and a fuel consumption of 8 g/s, the measured fuel-based specific impulse is 950 s.

## 6 Modified Design of the Thrust Module

To minimize the pressure loss in the internal path of the TM we have modified the design of the TM (Fig. 11*a*). Firstly, the prechamber for jet ignition of fuel–air mixture was made cylindrical and was moved from the bottom of the combustor to its axis (Fig. 11*b*). Secondly, the combustor of square  $100 \times 100$  mm<sup>2</sup> cross section was replaced by the cylindrical combustor 110 mm in diameter, so that the junction between the air intake with the combustor became smoother. Thirdly, the detonation tube 100 mm in diameter was replaced by the tube 110 mm in diameter, so that the junction of the combustor with the detonation tube became smoother. The tube length and the arrangement of turbulizing obstacles in the flame acceleration section were not changed. The air intake with the check valve was not changed as well. To improve the uniformity of fuel–air mixture in the combustor and for decreasing the fuel injection pressure, the number of fuel injectors was increased from 2 to 4.

Firing tests of the modified TM at the velocities of the approaching air flow  $V$  ranging from 25 to 65 m/s showed a significant improvement in thrust. The shaded area in Fig. 12 shows the values of mea-

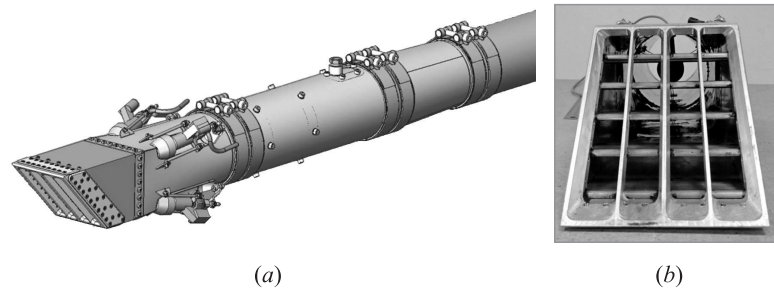


**Figure 11** Modified thrust module: (a) side view, and (b) front view

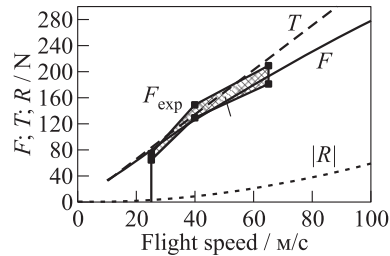


**Figure 12** Comparison of measured (shaded area) and calculated effective thrust  $F$  (solid curve) vs. flight speed for the 3-meter long TM with the detonation tube 110 mm in diameter. Dashed and dotted curves show the calculated full thrust  $T$  and aerodynamic drag  $R$  forces

sured effective thrust: now the effective thrust attained the maximum values of 180–200 N at  $V = 65$  m/s at the operation frequency of 8 Hz. The curves in Fig. 12 show the dependencies  $T(V)$ ,  $F(V)$ , and  $R(V)$  obtained with the use of formulae in Section 2 for the detonation tube with  $L = 3$  m and diameter 110 mm. It is seen that the measured values of the effective thrust correspond well to the estimates. Note that the specific impulse provided by the modified TM remained on the level of 1000 s.

The typical duration of firing tests of the modified TM was 300 s. Similar to the TM of the original configuration (see Fig. 4a), during this time the temperature of combustor walls in the modified TM attained a steady-state value not exceeding 200°C whereas the steady-state temperature of the turbulizing obstacles did not exceed 700 °C.

## 7 Catapult Launching Tests of an Unmanned Aerial Vehicle Powered with the Thrust Module

The modified TMs were used to power the UAVs with a take-off mass of up to 100 kg and perform their catapult launching short-duration flight tests. Figure 13 shows the UAVs powered by one TM (Fig. 13a) and two TMs (Fig. 13b) in the flight.

The difference from the US flight tests of the piloted Long E-Z aircraft powered by the multitube PDE, performed in 2008, is the natural (ram) rather than forced air supply into the engine. The results of catapult launching tests of UAVs have shown that the PDE-based power plants provide a subsonic flight with acceleration and



**Figure 13** The UAVs powered with one TM (a) and two paired TMs (b) in the flight

climbing. Due to the simplicity of design and low cost, as well as high propulsion performances, such power plants can be considered as an alternative to the propulsion units based on piston and turbojet engines for subsonic UAVs.

## 8 Concluding Remarks

Multivariant 3D calculations made it possible to design the TM for an aircraft intended for flight at a speed of 30 to 120 m/s when operating on a standard aviation kerosene TS-1. The TM consists of an intake with a check valve, a fuel supply system, a prechamber ignition system, and a combustor with a detonation tube attached. Parametric 3D calculations allowed choosing the best length of the combustor, which provides an efficient mixing of air with fuel, the best way to ignite the mixture (prechamber-jet ignition), the best location of the prechamber, the minimum length of the section with turbulizing obstacles for flame acceleration and DDT, and the best degree of filling the detonation tube with the fuel mixture to achieve the maximum completeness of combustion. The design of the TM in terms of the minimum pressure loss and the maximum thrust was not optimized.

The experimental sample of the TM was manufactured and its fire tests were performed on a test bench with a thrust-measuring table. In fire tests, TM characteristics are obtained in terms of the

dependencies of effective thrust, aerodynamic drag, and fuel-based specific impulse on fuel consumption at different speeds of the approaching air flow. The operation frequency of the TM was limited by the response time of the mechanical check valve: the maximum attained frequency was  $\sim 20$  Hz.

The measured values of the effective thrust of the TM turned out to be three times lower than the estimates based on the presumed values of the discharge coefficient of the intake. It is assumed that such a significant difference in the values of the effective thrust can be associated with the low discharge coefficient of the intake in the experimental sample of the TM: instead of the value of 0.5, adopted in the calculations, its real value is three times lower, i. e., close to 0.17. To increase the discharge coefficient of the intake and, consequently, the effective thrust, it is necessary to undertake measures for reducing the blockage of the intake section by the valve and other structural elements, i. e., to solve the task of optimizing the design of the inner path of the TM not only to ensure the operation process but also to minimize the pressure loss.

Modifications in the geometry of the inner path of the TM aimed at minimizing the pressure loss resulted in a significant increase of the thrust and the correspondence of the thrust values to the estimates based on the presumed values of the discharge coefficient. The maximum value of thrust attained the value of 180–200 N, while the fuel-based specific impulse was at the level of  $\sim 1000$  s.

The results of catapult launching tests of UAVs with power plants based on one and two paired TMs are presented. The world's first autonomous flight of an UAV with a new type of ramjet power plant is demonstrated. The results of catapult launching tests have shown that the PDE-based power plants provide a subsonic flight with acceleration and climbing. Due to the simplicity of design and low cost, as well as high propulsion performances, such power plants can be considered as an alternative to the propulsion units based on piston and turbojet engines for subsonic UAVs.

## Acknowledgments

This work was partly supported by the subsidy given to the N. N. Semenov Institute of Chemical Physics of the Russian Academy of

Sciences to implement the state assignment on the topic No.0082-2016-0011 “Fundamental studies of conversion processes of energetic materials and development of scientific grounds of controlling these processes” (Registration No. AAAA-A17-117040610346-5).

This work was supported by the Russian Science Foundation (Project No.14-13-00082P).

## References

1. Zel'dovich, Ya. B. 1940. K voprosu ob energeticheskom ispol'zovanii detonatsionnogo goreniya [To the question of energy use of detonative combustion]. *Sov. J. Techn. Phys.* 10(17):1455–1461.
2. Voitsekhovskii, B. V. 1959. Statsionarnaya detonatsiya [Stationary detonation]. *Dokl. USSR Acad. Sci.* 129(6):1254–1256.
3. Bykovskii, F. A., and S. A. Zhdan. 2013. *Nepreryvnaya spinovaya detonatsiya* [Continuous spin detonation]. Novosibirsk: Siberian Branch of the Russian Academy of Sciences Publ. 423 p.
4. Frolov, S. M., ed. 2006. *Impul'snye detonatsionnye dvigateli* [Pulsed detonation engines]. Moscow: TORUS PRESS. 592 p.
5. Frolov, S. M., V. S. Ivanov, I. O. Shamshin, and V. S. Aksenov. 2017. Tests of the pulsed-detonation ramjet model in a free air jet with Mach number up to 0.85. *Goren. Vzryv (Mosk.) — Combustion and Explosion* 10(3):43–52.
6. Zangiev, A. E., V. S. Ivanov, and S. M. Frolov. 2016. Thrust characteristics of an air-breathing pulse detonation engine in flight at Mach numbers of 0.4 to 5.0. *Russ. J. Phys. Chem. B* 10(2):272–283.
7. Belyaev, A. A., V. Ya. Basevich, and S. M. Frolov. 2015. Baza dannykh dlya rascheta laminarnogo i turbulentnogo goreniya vozdukhnykh smesey aviatsionnogo kerosina [Database for calculating laminar and turbulent combustion of aviation kerosene–air mixtures]. *Goren. Vzryv (Mosk.) — Combustion and Explosion* 8(1):29–36.
8. Basevich, V. Ya., A. A. Belyaev, S. N. Medvedev, V. S. Posvyanskii, and S. M. Frolov. 2015. Kineticheskiy detal'nyy i global'nyy mekhanizmy dlya surrogatnogo topliva [Detailed and global kinetic mechanisms for surrogate fuel]. *Goren. Vzryv (Mosk.) — Combustion and Explosion* 8(1):21–28.
9. Frolov, S. M. 2008. Fast deflagration-to-detonation transition. *Russ. J. Phys. Chem. B* 2(3):442–455.